

## Binary collision-induced light scattering by isotropic molecular gases

### II. Molecular spectra and induced rotational Raman scattering

by D. P. SHELTON† and G. C. TABISZ

Department of Physics, University of Manitoba,  
Winnipeg, Manitoba, Canada, R3T 2N2

(Received 26 July 1979)

The two-body collision-induced scattering spectra of  $\text{CH}_4$ ,  $\text{CD}_4$ ,  $\text{CF}_4$  and  $\text{SF}_6$  are presented. They are shown to contain features due to collision-induced rotational Raman scattering (CIRS). The spectra are used to obtain estimates of the magnitude of the molecular polarizabilities **A** (dipole-quadrupole) and **E** (dipole-octopole). The zeroth moment of the translational CIS spectrum also provides further evidence that the pair polarizability  $\beta(r)$  may be accurately described by the point dipole-induced-dipole (DID) model with small dispersion corrections.

#### 1. INTRODUCTION

In paper I of this series [1], the phenomenon of collision-induced light scattering is discussed and the experimental aspects of the present study are described. The spectrum of argon is analysed for two reasons: (i) to detail a newly confirmed feature, namely an excess of intensity over predictions of the first order dipole-induced-dipole (DID) model and (ii) to provide a basis for identification of spectral features distinctive to molecular spectra as compared to inert gas spectra. Here the molecular spectra are given and it is shown that features due to collision-induced rotational Raman transitions occur. A mechanism which accounts for their appearance can be described in terms of high-order molecular polarizabilities, such as the dipole-quadrupole and dipole-octopole polarizabilities, **A** and **E** respectively, [2]; the theory of this effect has been given by Buckingham and Tabisz [3, 4]. The present spectra are used to obtain estimates of the magnitudes of these polarizabilities.

#### 2. EXPERIMENTAL DETAILS

The molecular spectra are recorded and analysed as described in §§ 2 and 3 in [1]. The gases studied are  $\text{CH}_4$ ,  $\text{CD}_4$ ,  $\text{CF}_4$  and  $\text{SF}_6$ ; all samples except  $\text{CD}_4$  are supplied by Matheson. The  $\text{CH}_4$  is of 99.97 mol per cent purity. The  $\text{SF}_6$  contains a 0.06 mol per cent impurity of  $\text{O}_2$ . The  $\text{CF}_4$  as supplied has a 0.2 mol per cent impurity of air; this is reduced to 0.05 mol per cent by

† Present address: Department of Theoretical Chemistry, University Chemical Laboratory, Lensfield Road, Cambridge, CB2 1EW, England.

repeated melting and freezing of the  $\text{CF}_4$  and prolonged pumping on the liquid held in a bath at liquid oxygen temperature.  $\text{CD}_4$  is obtained from Merck, Sharpe and Doehme with an isotopic purity of 99 per cent. Unfortunately, a small leak in our sample handling apparatus resulted in a contamination of the sample by 0.8 mol per cent of air. Fractional distillation would result in too large a loss of  $\text{CD}_4$  to be economically feasible. The measurements are made at 295 K. The zeroth spectral moment of  $\text{CCl}_4$  vapour at 363 K and 1.3 atm has also been measured. The PVT data used in the analysis are given in [5].

### 3. THE SPECTRAL DATA

The two and three body spectra are obtained as described in [1]. The total intensities expressed as the zeroth spectral moments  $\phi^{(0)}/\text{\AA}^9$  are as follows:

$$\text{CH}_4: \phi^{(0)}/\text{\AA}^9 = 285 - 23.8 (\rho/\text{mol l}^{-1}),$$

$$\text{CF}_4: \phi^{(0)}/\text{\AA}^9 = 266 - 16.9 (\rho/\text{mol l}^{-1}),$$

$$\text{SF}_6: \phi^{(0)}/\text{\AA}^9 = 1166 - 329 (\rho/\text{mol l}^{-1}),$$

$$\text{CCl}_4: \phi^{(0)}/\text{\AA}^9 = 19.900.$$

The uncertainties are  $\pm 7$ , 10, 15 and 30 per cent increasing from  $\text{CH}_4$  to  $\text{CCl}_4$ . The two-body spectra are shown for  $\text{CH}_4$ ,  $\text{CD}_4$ ,  $\text{CF}_4$  and  $\text{SF}_6$  in figures 1, 2, 3

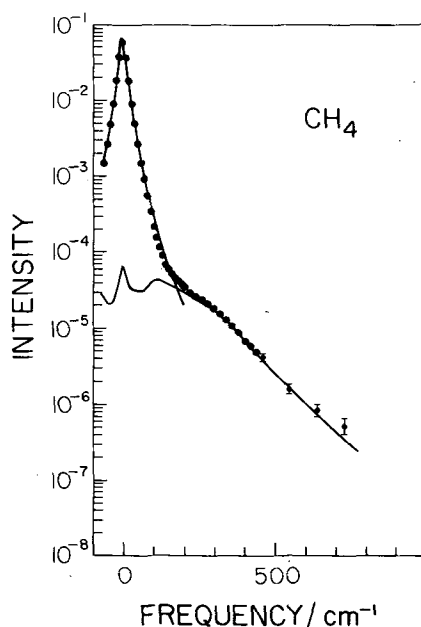


Figure 1. Comparison of the experimental and calculated spectrum of  $\text{CH}_4$ . The experimental spectrum is indicated by  $\bullet\bullet\bullet$  plotted every  $10\text{ cm}^{-1}$  to  $200\text{ cm}^{-1}$ , every  $20\text{ cm}^{-1}$  to  $460\text{ cm}^{-1}$  and at  $550$ ,  $640$  and  $730\text{ cm}^{-1}$ . The upper solid line is the calculated CIS spectrum with  $\beta(x) = x^{-3}$ . The lower line is the calculated CIRS spectrum with  $A = 1.0\text{ \AA}^4$  and  $E = -2.5\text{ \AA}^5$ . The intensity scale is the scattering cross-section relative to that of the  $\text{H}_2 S(1)$  line.

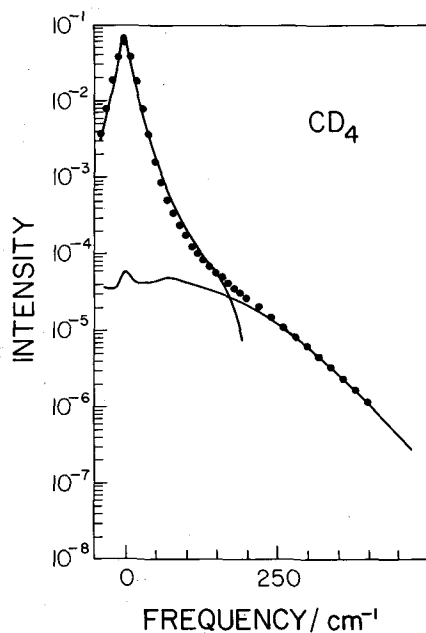


Figure 2. Comparison of the experimental and calculated spectrum of  $\text{CD}_4$ . The experimental spectrum is indicated by  $\bullet\bullet\bullet$  plotted every  $10\text{ cm}^{-1}$  to  $200\text{ cm}^{-1}$  and every  $20\text{ cm}^{-1}$  thereafter. The upper solid line is the calculated CIS spectrum with  $\beta(x) = x^{-3}$ . The lower line is the calculated CIRS spectrum with  $A = 1.0\text{ \AA}^4$  and  $E = -2.5\text{ \AA}^5$ .

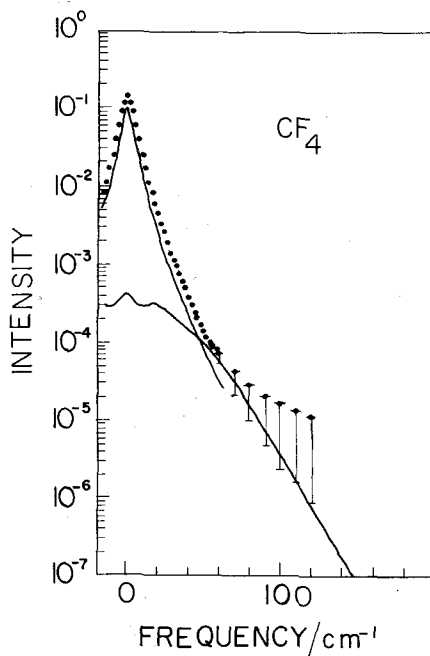


Figure 3. Comparison of the experimental and calculated spectrum of  $\text{CF}_4$ . The experimental spectrum ( $\bullet\bullet\bullet$ ) is plotted every  $2\text{ cm}^{-1}$  to  $60\text{ cm}^{-1}$  and every  $10\text{ cm}^{-1}$  thereafter. The upper curve is the calculated CIS spectrum with  $\beta(x) = x^{-3}$ . The lower curve is the calculated CIRS spectrum with  $A = 2.2\text{ \AA}^4$  and  $E = -2.2\text{ \AA}^5$ .

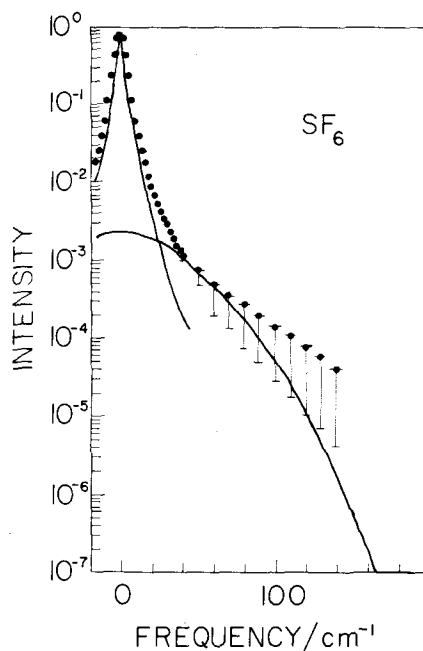


Figure 4. Comparison of the experimental and calculated spectrum of  $\text{SF}_6$ . The experimental spectrum ( $\bullet\bullet\bullet$ ) is plotted every  $2\text{ cm}^{-1}$  to  $40\text{ cm}^{-1}$  and every  $10\text{ cm}^{-1}$  thereafter. The upper curve is the calculated CIS spectrum with  $\beta(x)=x^{-3}$ . The lower curve is the calculated CIRS spectrum with  $A=0$  and  $E=20\text{ \AA}^5$ .

and 4 respectively. Also plotted are computed spectra based on a first order DID model for the pair polarizability anisotropy,  $\beta(x)=x^{-3}$  where  $x=r/\sigma$ ,  $r$  is the intermolecular separation and  $\sigma$  is the molecular diameter. The sharp downward turn of the  $\text{CH}_4$  and  $\text{CD}_4$  calculated profiles at about  $150\text{ cm}^{-1}$  is spurious and due to an artefact of the calculation. See the description of the calculation in § 5 of [1]. As with argon, these computed spectra generally agree in shape with those observed at low and intermediate frequency shift regions; for  $\text{CF}_4$  and  $\text{SF}_6$  the calculated spectral intensities are uniformly too low because of the potentials chosen for the calculation. At high frequency an abrupt change in shape occurs for all molecules, for which the DID model cannot account at all. The two-body intensities are summarized in table 1 together with  $\phi^{(0)}/\text{\AA}^9$  calculated using a first order DID model ( $\beta(r)=6\alpha^2/r^3$ , where  $\alpha$  is the molecular polarizability). The observed intensity generally exceeds the calculated value.

In the remainder of this paper, it is argued that the change of shape at high frequency and a portion of the excess intensity is due to a mechanism other than translational collision-induced scattering (CIS), which is all that can occur in the case of argon. This additional mechanism is collision-induced rotational Raman scattering (CIRS). The surmise about the nature of the high frequency tail may be confirmed by an experiment involving an isotopic substitution. The frequency spread of the translational spectrum is essentially determined by the molecular diameter and velocity. The width of the CIRS spectrum on the other hand depends on a rotational constant and hence the moment of inertia of

Table 1. Zeroth moments of the spectra.

	$\phi_{\text{expt}}^{(0)}/\text{\AA}^9$	$\phi_{\text{CIRS}}^{(0)}/\text{\AA}^9$	$\phi_{\text{calc}}^{(0)}/\text{\AA}^9$ (b) (first order)	K (c)	$\phi_{\text{calc}}^{(0)}/\text{\AA}^9$ (d)	$\frac{\phi_{\text{expt}}^{(0)} - \phi_{\text{CIRS}}^{(0)}}{\phi_{\text{calc}}^{(0)}}$
Ar (a)	50.9	—	46.6 (e)	1.29	50.1 (e)	1.01 (o)
CH <sub>4</sub> (a)	285	3.5	253 (f)	1.21	274 (f)	1.03 (o)
CF <sub>4</sub> (a)	266	7	252 (g) 162 (h)	1.05	264 (g) 166 (h)	0.98 1.56 (o)
CCl <sub>4</sub> (a)	19900	—	24600 (i) 16700 (j)	1	26100 (i) 17700 (j)	0.76 1.12
SF <sub>6</sub> (a)	1166	60	1397 (k) 1070 (l) 909 (m) 579 (n)	1.02	1477 (k) 1119 (l) 948 (m) 642 (n)	0.75 0.99 1.17 1.72 (o)

(a) The polarizabilities at 4880 Å are : Ar,  $\alpha = 1.679 \text{ \AA}^3$  [9]; CCl<sub>4</sub>,  $\alpha = 10.59 \text{ \AA}^3$  [11]; CH<sub>4</sub>,  $\alpha = 2.642 \text{ \AA}^3$  [10]; SF<sub>6</sub>,  $\alpha = 4.549 \text{ \AA}^3$  [10]; CF<sub>4</sub>,  $\alpha = 2.937 \text{ \AA}^3$  [10].

(b)  $\phi^{(0)}/\text{\AA}^9 = 4\pi(36\alpha^4/\sigma^3) \int_0^\infty dx x^{-4} g(x)$  where  $x = r/\sigma$  and  $g(x) = \exp(-V(x)/kT)$ .

(c) See [16, chap. 2].

(d)  $\phi^{(0)}/\text{\AA}^9 = 4\pi(36\alpha^4/\sigma^3) \left[ \int_0^\infty dx x^{-4} g(x) + 2K(\alpha/\sigma^3) \int_0^\infty dx x^{-7} g(x) \right]$ .

(e) Smith's potential  $\epsilon/k = 142.1 \text{ K}$ ,  $\sigma = 3.35 \text{ \AA}$  [17].

(f) 6-20 potential  $\epsilon/k = 217 \text{ K}$ ,  $\sigma = 3.557 \text{ \AA}$  [18].

(g) 7-28 potential  $\epsilon/k = 288 \text{ K}$ ,  $\sigma = 4.20 \text{ \AA}$  [19].

(h) 6-12 potential  $\epsilon/k = 152.5 \text{ K}$ ,  $\sigma = 4.70 \text{ \AA}$  [20].

(i) 7-28 potential  $\epsilon/k = 683.2 \text{ K}$ ,  $\sigma = 6.03 \text{ \AA}$  [21].

(j) 6-12 potential  $\epsilon/k = 327 \text{ K}$ ,  $\sigma = 5.88 \text{ \AA}$  [22].

(k) 7-28 potential  $\epsilon/k = 439 \text{ K}$ ,  $\sigma = 4.68 \text{ \AA}$  [19].

(l) 7-28 potential  $\epsilon/k = 414 \text{ K}$ ,  $\sigma = 5.03 \text{ \AA}$  [23].

(m) 6-12 potential  $\epsilon/k = 259 \text{ K}$ ,  $\sigma = 5.01 \text{ \AA}$  [24].

(n) 6-12 potential  $\epsilon/k = 200.9 \text{ K}$ ,  $\sigma = 5.51 \text{ \AA}$  [20].

(o) The potentials (e), (f), (h) and (n) have been used to calculate the DID spectra of figures 1, 2, 3 and 4.

the molecule (§ 4). Consider the pair of molecules CH<sub>4</sub> and CD<sub>4</sub> with masses 16  $m_u$  and 20  $m_u$  respectively. The velocity of a CD<sub>4</sub> molecule at a given temperature will be  $(16/20)^{1/2}$  or 0.89 times that of a CH<sub>4</sub> molecule with the same energy. Other relevant properties of these molecules such as their polarizability, diameter and intermolecular potential are essentially identical [6]. Except for a slight decrease in width (steepening of the slope of the profile), the CD<sub>4</sub> translational CIS spectrum should be similar to that of CH<sub>4</sub>. On the other hand, the moment of inertia of CD<sub>4</sub> is twice as large as that of CH<sub>4</sub>; consequently the rotational constant B (table 2) will be half as large. The frequency of all rotational transitions for CD<sub>4</sub> will be reduced by a factor of two from the frequencies of CH<sub>4</sub> rotational transitions and so the entire CIRS spectrum will be shifted down in frequency by a factor of two. The spectra of CH<sub>4</sub> and CD<sub>4</sub> obtained under the same conditions are compared in figure 5. At small frequency shifts the two spectra are almost identical. The high

Table 2. Collision-induced rotational scattering : molecular constants.

	$B/\text{cm}^{-1}$	$A/\text{\AA}^4$		$E/\text{\AA}^5$	
		Model†	Expt.‡	Model†	Expt.‡
$\text{CH}_4$	5.25	1.0, 0.82§	$1.0 \pm 0.1$	-1.0	$2.5 \pm 0.2$
$\text{CD}_4$	2.63	1.0	$1.0 \pm 0.1$	-1.0	$2.5 \pm 0.2$
$\text{CF}_4$	0.185	2.2	2.2		10
$\text{SF}_6$	0.087	0		20	20

† Calculated from the bond polarizability model, see [4].

‡ Only the magnitude and not the sign may be determined from the present experiments.

§ *Ab initio* calculation, averaged in the ground vibrational state, dispersion correction between zero frequency and 4880 Å estimated and applied, [8].

|| Upper bound.

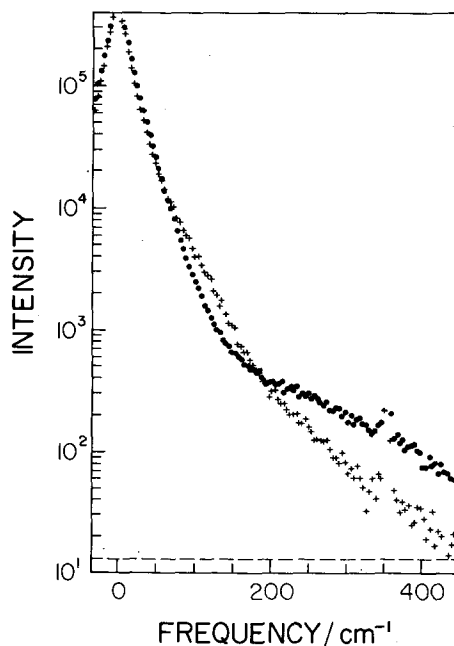


Figure 5. Comparison of the  $\text{CH}_4$  and  $\text{CD}_4$  spectra. The  $\text{CH}_4$  spectrum is indicated by ●●● and that of  $\text{CD}_4$  by + + +. The background count rate is shown by - - -. The sharp peak at  $354 \text{ cm}^{-1}$  is the  $S(0)$  line of  $\text{H}_2$ . The upward bulge in the  $\text{CD}_4$  spectrum between  $60$  and  $180 \text{ cm}^{-1}$  is due to contamination of the sample by air. The pressure is  $75 \text{ atm}$  and the spectral slit width is  $3 \text{ cm}^{-1}$ .

frequency tails are, however, drastically different. This is the clear signature of the contribution of CIRS to the  $\text{CH}_4$  and  $\text{CD}_4$  spectra.

Having demonstrated that CIRS does indeed occur in the molecular spectra, it is desirable to compare computed and observed spectra to obtain more quantitative information. Before doing so, a review of the theory of CIRS will be helpful.

## 4. COLLISION-INDUCED ROTATION RAMAN SCATTERING

The theory of CIRS due to long-range interactions has been given in detail earlier [3, 4]; the following is a brief summary. In a weak non-uniform electric field  $\mathbf{F}$ , the total dipole of a molecule may be written as :

$$\mu_\alpha = \mu_\alpha^{(0)} + \alpha_{\alpha\beta} F_\beta + \frac{1}{3} A_{\alpha\beta\gamma} F'_{\beta\gamma} + \frac{1}{15} E_{\alpha\beta\gamma\delta} F''_{\beta\gamma\delta} + \dots, \quad (1)$$

where  $\mu_\alpha^{(0)}$  is the  $\alpha$  component of the permanent dipole moment,  $\alpha_{\alpha\beta}$  is the  $\alpha\beta$  component of the dipole polarizability,  $A_{\alpha\beta\gamma}$  is the  $\alpha\beta\gamma$  component of the dipole-quadrupole polarizability,  $E_{\alpha\beta\gamma\delta}$  is the  $\alpha\beta\gamma\delta$  component of the dipole-octopole polarizability, and  $F'_{\beta\gamma}$  and  $F''_{\beta\gamma\delta}$  are the  $\beta\gamma$  and  $\beta\gamma\delta$  components of the field gradients. For the tetrahedral and octahedral molecules of the present study,  $\mu^{(0)} = 0$ ;  $\mathbf{A}$  is also zero for octahedral molecules. For tetrahedra, the magnitude of  $\mathbf{A}$  may be expressed by a single parameter  $A$  and for both species that of  $\mathbf{E}$  by a parameter  $E$ . When two identical molecules interact, each is in the dipole field of the other plus the field of the external light beam. Then the mean square pair polarizability is :

$$\langle \alpha_{zz}^2 \rangle = (4\alpha)^2 + \frac{16}{5} a^4 r^{-6} + \frac{1184}{105} (\alpha^2 A^2) r^{-8} + \frac{95616}{4725} A^4 r^{-10} + \frac{194}{9} \alpha^2 E^2 r^{-10} + \dots, \quad (2)$$

$$\langle \alpha_{xz}^2 \rangle = \frac{12}{5} \alpha^4 r^{-6} + \frac{96}{35} \alpha^2 A^2 r^{-8} + \frac{62912}{4725} A^4 r^{-10} + \frac{22}{9} \alpha^2 E^2 r^{-10} + \dots \quad (3)$$

In the present experiment,  $\langle \alpha_{xz}^2 \rangle$  is the important quantity, measuring the square of the pair anisotropy relative to space fixed axes.  $\langle \dots \rangle$  denotes an average over all orientations of 1 and 2 and of the intermolecular axis. The term in  $r^{-6}$  is the first order DID contribution; those in  $r^{-8}$  and  $r^{-10}$  yield the rotational scattering.  $\beta(r)$  is measured in the molecular frame and  $\langle \alpha_{xz}^2 \rangle$  in the laboratory frame; consequently the coefficients of the DID terms are different in the two cases. The terms in  $(\alpha A)^2$  lead to the selection rule  $\Delta J = 0, \pm 1, \pm 2, \pm 3$  where  $J$  is the total angular momentum quantum number of one of the molecules; those in  $(\alpha E)^2$  follow  $\Delta J = 0, \pm 1, \pm 2, \pm 3, \pm 4$ ; the terms  $A^4$  correspond to double rotational transitions where each molecule of the pair can make the transitions  $\Delta J = 0, \pm 1, \pm 2, \pm 3$ .

## 5. COMPARISON WITH EXPERIMENT

With the use of this theory, it is possible to compute spectra. For a direct comparison with experiment the magnitudes of the tensors  $\mathbf{A}$  and  $\mathbf{E}$  must be known. They may be estimated from a bond polarizability model given by Buckingham [2, 7] (see table 2). An  $XY_n$  molecule, is represented by  $n$  anisotropically polarizable groups each one symmetric about its  $XY$  bond. For tetrahedral molecules  $A = (4/\sqrt{3})(\alpha_{\parallel} - \alpha_{\perp})R_0$  and  $E = -(8/3)(\alpha_{\parallel} - \alpha_{\perp})R_0^2$ ;  $E = 6(\alpha_{\parallel} - \alpha_{\perp})R_0^2$  for octahedral molecules;  $(\alpha_{\parallel} - \alpha_{\perp})$  is the polarizability anisotropy of  $Y$  and  $R_0$  is the distance from the centre of the molecule. Details of the computation of the spectra are given in [4]. A rigid rotor model is

assumed and the broadening of each rotational transition is approximated by the pure translational profile, that is the shape of the low frequency shift CIS spectrum. The computed spectra are shown in figures 1, 2, 3 and 4 together with the experimental data and DID predictions. The total intensity of the CIRS spectra are 1.2, 2.5 and 5 per cent of the total spectral intensity for  $\text{CH}_4$ ,  $\text{CF}_4$  and  $\text{SF}_6$  respectively. For both  $\text{CH}_4$  and  $\text{CD}_4$ , the computed CIRS spectrum agrees very well with the observed high frequency tail. In the cases of  $\text{CF}_4$  and  $\text{SF}_6$ , the results are less satisfactory; the translational and rotational CIS spectra are not so clearly separated as with  $\text{CH}_4$ , and the observed intensity at large frequency shifts is much greater than accounted for by the present calculation. Double rotational transitions involving the polarizability **E** produce a broader spectrum than that due to double **A** transitions, but with the values of *A* and *E* estimated for  $\text{CF}_4$  using the bond polarizability model, the contribution of single and double **E** transitions to the overall CIRS spectrum is small. However, by assuming a larger value of *E* the agreement between the calculated and measured spectrum can be improved for  $\text{CF}_4$ . Even though the CIRS spectrum is not cleanly separated from the translational CIS spectrum it is possible to establish experimental upper bounds on the magnitudes of *A* and *E*. The upper bound of *A* is the largest value such that the calculated intensity does not exceed that measured at any frequency. Except for molecules such as  $\text{CH}_4$ ,  $\text{SiH}_4$  or  $\text{GeH}_4$ , more accurate estimates of *A* and *E* derived from measured CIS spectra will require accurate estimates of the corresponding translational CIS spectra. For  $\text{SF}_6$  the CIRS spectrum is dominated by double **E** transitions when the bond polarizability value of *E* is assumed. To account for the excess intensity at large frequency shifts in this case it seems that we must invoke the next higher order polarizability tensor.

The magnitudes of *A* and *E* estimated from this analysis are listed in table 2. These values differ from those of references [3] and [4]. The reason is that in [3] and [4] all the excess intensity over the first order DID predictions was ascribed to CIRS. Our study of argon [1] demonstrated that even for the inert gases the CIS intensity is greater than such predictions and at least second order DID effects appear. Therefore in the present study we have elected to work with the CIRS profile in the realization that such DID effects must affect the intensity for the molecules as well. These effects form the subject of the next section of this paper.

Before ending the discussion of CIRS, a cautionary remark must be made. The comparison of the  $\text{CH}_4$  and  $\text{CD}_4$  spectra demonstrates the presence of induced rotational transitions. It does not, however, provide evidence that the present explanation in terms of the polarizabilities, **A**, **E**, etc. is unique. Short-range interactions could result in the breakdown of molecular symmetry and give rise to the same rotational selection rules and spectral profile. Confidence in the present discussion in terms of a long-range interaction is derived from the reasonable values of *A* and *E* obtained.

## 6. TRANSLATIONAL CIS

Let us now return to the translational CIS spectrum and modifications to the DID model. Similar considerations were made regarding the spectrum of argon in [1]. Even when the contributions of CIRS are accounted for, an



excess of intensity remains over the predictions of the first order DID model. In the classical point DID model, the polarizability anisotropy is given by [12]

$$\beta(x) = x^{-3} + (\alpha/\sigma^3)x^{-6} + \dots, \quad (4)$$

where  $\beta(r) = (6\alpha^2/\sigma^3)\beta(x)$  and  $x = r/\sigma$ . Buckingham and Clark have derived an expression for the  $x^{-6}$  term of  $\beta(x)$  based on a model which includes the second hyperpolarizability  $\gamma$  of the molecules [15]. The results of this model agree very well with quantum mechanical perturbation calculations for  $(\text{H})_2$  [13] and  $(\text{He})_2$  [14]. The coefficient of the  $x^{-6}$  term has the value  $K(\alpha/\sigma^3)$  where

$$K = 1 - \gamma C_6/18\alpha^4 \quad (5)$$

and  $C_6$  is the coefficient of the  $r^{-6}$  term in the dispersion interaction energy of two molecules. The coefficient  $K$  tends to unity for larger, more polarizable molecules and so  $\beta(x)$  tends to the classical point DID model. The values of  $\phi^{(0)}/\text{\AA}^9$  calculated using

$$\beta(x) = x^{-3} + K(\alpha/\sigma^3)x^{-6} \quad (6)$$

are compared with the measured values for several molecules in table 1. For Ar and  $\text{CH}_4$  the agreement is excellent. The comparison for  $\text{CF}_4$ ,  $\text{CCl}_4$  and  $\text{SF}_6$  is complicated by the fact that the intermolecular potential is not known so accurately for these molecules. The calculated value of  $\phi^{(0)}/\text{\AA}^9$  is quite sensitive to the diameter  $\sigma$  of the repulsive core of the potential. The most discrepant values of  $\phi_{\text{calc}}^{(0)}/\text{\AA}^9$  correspond to those potentials (labelled  $h$  and  $n$ ) where the parameter  $\sigma$  may be judged to be too large. Considering the remaining values of  $\phi_{\text{calc}}^{(0)}/\text{\AA}^9$  we see that they are in significant agreement with the experimental values. This concurs with the theoretical findings. Recent calculations indicate that the electron overlap mechanism makes only a small contribution to the total intensity (see [1] part 4). Also, Clarke [16] has shown that the distribution of polarizable matter within the molecule does not result in significant deviations from the results of the point DID model for  $\text{SF}_6$ , using a calculation based on the atom-atom approximation. Higher order DID terms probably increase  $\phi^{(0)}/\text{\AA}^9$  by a few per cent but are cancelled by the electron overlap contribution. (The electron overlap term may also alter the spectral shape at large frequency shifts significantly.) Consideration of the intensity of the CIS spectrum strongly favours the point DID model with minor corrections.

Comparisons of our calculated and measured spectral shapes are also consistent with a long-range DID form for  $\beta(x)$ . However, the classical correlation function used in the present computation of the CIS spectrum yields its best results at intermediate frequency shifts. At small frequency shifts the contribution of bound dimers is not properly accounted for while at large frequency shifts the velocity change of the colliding molecules during the scattering event is not accounted for. Thus, in order to draw quantitative conclusions about  $\beta(x)$  from the spectral shape one must resort to a quantum mechanical calculation.

This work was supported by grants from the National Research Council of Canada and the Research Corporation (New York).

## REFERENCES

- [1] SHELTON, D. P., and TABISZ, G. C., 1980, *Molec. Phys.*, **40**, 285.
- [2] BUCKINGHAM, A. D., 1967, *Adv. chem. Phys.*, **12**, 107.
- [3] BUCKINGHAM, A. D., and TABISZ, G. C., 1977, *Optics Lett.*, **1**, 220.
- [4] BUCKINGHAM, A. D., and TABISZ, G. C., 1978, *Molec. Phys.*, **36**, 583.
- [5] DOUSLIN, D. P., HARRISON, R. H., and MCCULLOUGH, J. P., 1964, *J. chem. Engng. Data*, **9**, 358 and 1961, *J. chem. Phys.*, **35**, 1357. MACCORMACK, K. E., and SCHNEIDER, W. G., 1951, *J. chem. Phys.*, **19**, 845. LAMBERT, J. D., ROBERTS, G. A. H., ROWLINSON, J. S., and WILKINSON, V. J., 1949, *Proc. R. Soc. A*, **196**, 113.
- [6] THOMAES, G., and VAN STEENWINKEL, R., 1962, *Molec. Phys.*, **5**, 307.
- [7] BUCKINGHAM, A. D., 1970, *Physical Chemistry, An Advanced Treatise*, Vol. 4, edited by H. Eyring, W. Jost and D. Henderson (Academic Press), Chap. 8.
- [8] AMOS, R. D., 1979, *Molec. Phys.*, **38**, 33.
- [9] DALGARNO, A., and KINGSTON, A. E., 1960, *Proc. R. Soc. A*, **259**, 424.
- [10] WATSON, H. E., and RAMASWAMY, K. L., 1936, *Proc. R. Soc. A*, **156**, 144.
- [11] LANDOLT-BORNSTEIN, 1962, *Zahlenwerte und Funktionen*, Band II, Teil 8 (Springer).
- [12] SILBERSTEIN, L., 1917, *Lond. Edinb. Dubl. Phil. Mag.*, **33**, 92, 521.
- [13] BUCKINGHAM, A. D., MARTIN, P. H., and WATTS, R. S., 1971, *Chem. Phys. Lett.*, **21**, 186.
- [14] CERTAIN, P. J., and FORTUNE, P. R., 1971, *J. chem. Phys.*, **55**, 5818.
- [15] BUCKINGHAM, A. D., and CLARKE, K. L., 1979, *Chem. Phys. Lett.*, **57**, 321.
- [16] CLARKE, K., 1978, *Molecular Property Densities and Pair Polarizabilities* (Ph.D. Thesis), (Cambridge, U.K.), Chap. 5.
- [17] SMITH, E. B., 1974, *Physica*, **73**, 211.
- [18] MATTHEWS, G. P., and SMITH, E. B., 1976, *Molec. Phys.*, **32**, 1719.
- [19] MCCOUBREY, J. C., and SINGH, N. M., 1959, *Trans. Faraday Soc.*, **55**, 1926.
- [20] MACCORMACK, K. E., and SCHNEIDER, W. G., 1951, *J. chem. Phys.*, **19**, 849.
- [21] DAVID, H. G., HAMANN, S. D., and THOMAS, K. B., 1954, *Aust. J. Chem.*, **12**, 309.
- [22] HIRSCHFELDER, J. O., CURTISS, C. F., and BIRD, R. B., 1954, *Molecular Theory of Gases and Liquids* (Wiley), p. 1111.
- [23] HAMANN, S. D., and LAMBERT, J. A., 1954, *Aust. J. Chem.*, **7**, 1.
- [24] ELLIS, C. P., and RAW, C. J. G., 1959, *J. chem. Phys.*, **30**, 574.